

Interference diversity in frequency-hopped systems with soft decoding

Kostas Stamatiou and John G. Proakis

Department of Electrical & Computer Engineering

University of California San Diego, La Jolla, CA 92093-0407

Email: kostas@ucsd.edu, jproakis@cwc.ucsd.edu

Abstract—In this paper, we analyze the effect of interference diversity on the capacity of a cellular system that employs frequency hopping, power control and bit-interleaved coded modulation. Interference is created when the hopping patterns of adjacent cells intersect with the patterns of the cell of interest, with a probability that depends on the occupancy of each cell. However, due to frequency hopping and power control, the power of the interference varies randomly across the received symbols creating what is usually named in the literature as *interference diversity*. We explicitly take into account this randomness and, under a channel model that accounts for fading and path loss, analyze the performance of two receivers; a receiver that tracks the variations of the interference power across the received symbols and a receiver that remains oblivious to these variations. Our results demonstrate under what circumstances the additional complexity of tracking the interference power variations is justified.

I. INTRODUCTION

Frequency hopping (FH) combined with coding is a widely used technique at the physical layer of cellular systems. Frequency diversity is attained, if the channel frequency response varies over the hopping distance. More importantly, the inter-cell interference is “spread over” different users and no user is subject to worst case interference conditions. This effect is usually called *interference averaging (IA)* and the variation of the interference power across the received coded symbols, *interference diversity (ID)*.

ID is the result of FH, since some time/frequency slots are interfered and some are not, depending on the system load. However, even in a fully loaded system, ID is present if the interfering users are power controlled. Knowledge of the interference power at each received symbol can improve the reliability of the respective decoder metric and thus the overall error performance. This is similar to exploiting channel state information in a single-user fading channel (coherent vs. non-coherent detection) or the knowledge of unreliable symbols in errors-and-erasures decoding of Reed-Solomon codes [1]. The effect of ID is qualitatively analyzed in [2]. A specific construction of patterns that achieves perfect IA is described in [3] and more recently in [4]. Other related work on the topic includes [5], [6].

In this paper, we analyze the effect of ID on the capacity of a cellular system that employs FH, PC and bit-interleaved coded modulation (BICM). A channel model that includes the effects of fading and path-loss is assumed. The performance of two receivers is analytically evaluated; a receiver that tracks the interference power variations and one that doesn't. Our main conclusion is that, under small long-term signal-to-interference (SIR) ratios, which correspond to the user being situated close to the boundary of its cell, increasing the decoding complexity albeit ignoring the interference variations results in a small performance improvement. In other words, trading decoding complexity with an interference tracking capability can be more beneficial in terms of the error rate performance. A variety of numerical results are presented which illustrate this point.

The rest of the paper is structured as follows. In section II our system model is described. We proceed with the analysis in section III. Section IV includes the numerical results and section V concludes the paper.

II. SYSTEM DESCRIPTION

Consider the downlink of a synchronous cellular system which is slotted in time and frequency. For simplicity, assume there are only two circular cells with radius R_0 , a base-station $B_i, i = 0, 1$, at their center and uniformly distributed users. A user in the cell of B_0 is taken as a reference (user of interest, UI), thus the signals transmitted by B_1 generate interference to the link B_0 -UI. The selection of the downlink direction for the evaluation of the performance is arbitrary. The analysis can also be carried out in the uplink, with the proper modifications in the distributions of the random variables involved.

The bandwidth is divided into N flat-fading frequency bands or subcarriers (the term subcarriers is more appropriate in the context of a FH-OFDMA system, see [4], [7].) Each user is assigned a hopping pattern, which chooses a subcarrier in each time slot. We assume that the patterns within a cell are orthogonal, so that there is no intra-cell interference. However, if N_1 users are present in cell 1, then there is a probability of interference of any hopping pattern in that cell with the pattern assigned to UI, equal to $p = N_1/N$. It is also assumed that, within the span of the error events in the decoder of UI, the interference is due to different users. In other words, we are studying a scenario of complete interference randomization. A

construction of hopping patterns that fits this statistical model can be achieved with the help of Latin squares, as described in [3].

According to the basic BICM setup [8], the binary information stream to be transmitted by B_0 to UI is encoded by a convolutional encoder. The binary codeword c is interleaved and Gray-mapped to symbols from a M -QAM constellation, $M = 2^m$, yielding the symbol codeword x . At time k , each symbol, $x_{0,k}$ (normalized, such that $\mathbb{E}[|x_{0,k}|^2] = 1$) is transmitted on the subcarrier selected by the hopping pattern of UI. Under perfect PC, the received symbol, y_k , is given by

$$\begin{aligned} y_k &= \sqrt{\gamma}H_{0,k}x_{0,k} + \sqrt{\gamma R^{-b}r_k^b}\alpha_k e^{i\phi_k} H_{1,k}x_{1,k} + n_k \\ &= \sqrt{\gamma}H_{0,k}x_{0,k} + n'_k \end{aligned} \quad (1)$$

The different terms in (1) are as follows: γ denotes the received SNR, $H_{i,k} \sim \mathcal{CN}(0, 1)$ the fading coefficient from B_i to UI, $x_{i,k}$ the transmitted symbol from B_i and $n_k \sim \mathcal{CN}(0, 1)$ the additive noise. The power transmitted by B_1 is attenuated by the factor R^{-b} , where R is the distance between B_1 and UI and $b > 0$ is the path loss exponent. If D is the reuse distance, i.e. the distance between two base-stations in the cellular system using the same set of frequencies, then $R^2 = D^2 + r_0^2 - 2Dr_0\cos\theta$ (see fig. 1). The distance between B_1 and its user whose pattern may be scanning the same subcarrier as UI at time k is denoted with the lowercase r_k . The event of interference is modelled by the variable α_k , which is one (zero) with probability $p = N_1/N$ ($1 - p$). The random phase component $e^{i\phi_k}$ is present since there is no carrier synchronization between UI and B_1 ; it does not affect our analysis and can be absorbed in $H_{1,k}$. Finally, it is assumed that all random variables are independent across k .

Note that, with respect to a performance measure such as the bit-error-probability (BER), R is considered a ‘‘long-term’’ random variable, i.e. it is assumed constant within the interval that the performance is evaluated. This is due to the fact that its variation rate, which depends on how often the position of the user changes, is much smaller compared to the transmission rate. On the contrary, r_k, α_k are perceived as ‘‘fast’’ random variables by the decoder, since they change independently across k . This randomization is reflected on the instantaneous SINR, which is given by

$$\text{SINR}_k = \frac{1}{\beta r_k^b \alpha_k + \gamma^{-1}} = \frac{1}{\xi_k + \gamma^{-1}} \quad (2)$$

where ξ_k is the total interference power at time k and $\beta \triangleq R^{-b}$ can be regarded as the inverse of the *long-term* SIR.

This section is closed with a few words about the distributions of distance variables. Since the users are uniformly distributed, the probability density function (pdf) of the distance r of a user from its base-station is $f(r) = 2r/R_0^2$, $r \in (0, R_0]$, so the pdf of $r' = r^b$ is

$$f(r') = \frac{2}{bR_0^2} r'^{2/b-1}, \quad r' \in (0, R_0^b] \quad (3)$$

For convenience, we can make the normalization $R_0 = 1$, which reveals that r' is a Beta random variable with parameters

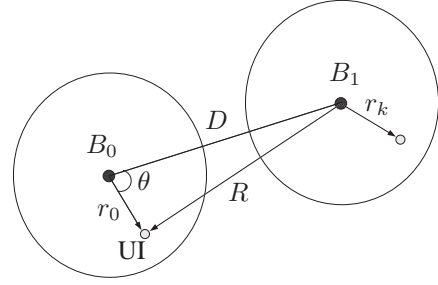


Fig. 1. Downlink scenario.

$(2/b, 1)$ [9]. The empirical pdf of $-10\log r'$ is shown in fig.2. The plot demonstrates the wide range of values that the interference power or, equivalently, $\text{SIR}_k = 1/(\beta r_k^b)$ can take, at any given time k .

III. PERFORMANCE ANALYSIS

A. Bit error probability of BICM

We consider two receivers, one that takes into account the variation of ξ_k across the received symbols (receiver 1 - R1) and one that doesn't (R2). Both R1 and R2 have perfect knowledge of the fading coefficients H_k (for an analysis of the performance with pilot-assisted channel estimation, see [7]) and, in addition, R1 has perfect knowledge of SINR_k . The criterion for deciding that the binary codeword c was transmitted is [8]

$$\hat{c} = \underset{c \in \mathcal{C}}{\text{argmin}} \left\{ \sum_k \min_{x \in \mathcal{X}_{c_k}^{i_k}} \left\{ \frac{|y_k - H_k x|^2}{w_k} \right\} \right\}$$

where the weighting factor w_k is $w_k = \text{SINR}_k^{-1} = \xi_k + \gamma^{-1}$ for R1 and $w_k = 1$ for R2. $\mathcal{X}_{c_k}^{i_k}$ denotes the set of constellation symbols that have bit c_k at position $i_k = 1, \dots, m$. The position i_k within x_k , in which the bit c_k was transmitted, i.e. the interleaving strategy, is known at the receiver. For the purpose of our analysis, we assume random interleaving.

The BER of both receivers can be approximated by

$$P_b \simeq \frac{1}{k_c} \sum_{L=d_{\min}}^{d_{\min}+K} e(L)P(L) \quad (4)$$

where k_c is the number of information bits per trellis branch, d_{\min} is the minimum Hamming distance, K is a positive integer of our choice, $e(L)$ is the total information-bit weight of error events at distance L and $P(L)$ is the pairwise error probability (PEP). Following [8], the PEP is upper-bounded by

$$P(L) \leq \frac{1}{2\pi i} \int_{\sigma-i\infty}^{\sigma+i\infty} \frac{1}{s} [\Phi(s)]^L ds \quad (5)$$

where

$$\Phi(s) = \frac{1}{m2^m} \sum_{i=1}^m \sum_{c=0}^1 \sum_{x \in \mathcal{X}_c^i} \Phi_{\Delta(x, x')} (s) \quad (6)$$

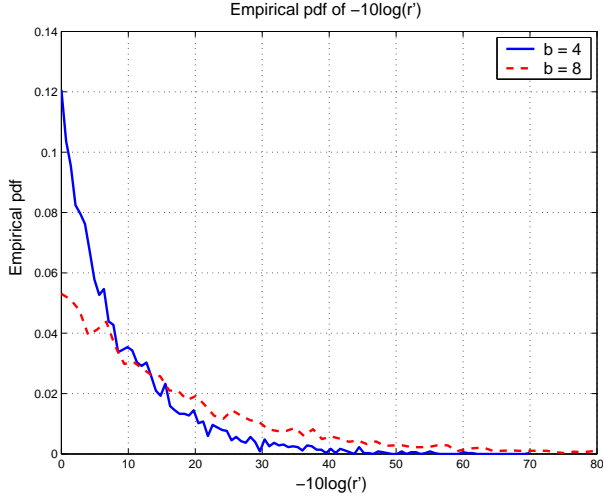


Fig. 2. Empirical pdf of $-10\log r'$. The pdf was computed over 5000 realizations.

with $\Phi_{\Delta(x,x')}(s)$ denoting the characteristic function of the random variable $\Delta(x,x') = \mathbf{z}^H \mathbf{Q} \mathbf{z}$, $\mathbf{z} = \frac{1}{w} [H(x-x') \ n']^T$ and x' being the closest neighbor of x that has the complementary bit \bar{c} in position i (note that, due to the assumption of independence across time, the subscript k has vanished.) The integral in (5) can be evaluated numerically by Gauss-Chebyshev quadrature [10] and we obtain

$$P(L) \leq \frac{1}{N} \sum_{n=1}^{N/2} \text{Re}\{[\Phi(\epsilon + j\epsilon\tau_n)]^L\} + \tau_n \text{Im}\{[\Phi(\epsilon + j\epsilon\tau_n)]^L\}$$

where $\tau_n = \tan(\frac{(2n-1)\pi}{2N})$, N is the number of nodes and ϵ must belong to the region of convergence of $\Phi(s)$.

B. Evaluation of $\Phi_{\Delta(x,x')}(s)$

From the rule of conditional expectation we have that

$$\Phi_{\Delta(x,x')}(s) = \mathbb{E}_\alpha [\Phi_{\Delta(x,x')|\alpha}(s)] = \mathbb{E}_\alpha [\mathbb{E}_{\xi|\alpha} [\Phi_{\Delta(x,x')|\xi}(s)]]$$

or, since α is a Bernoulli random variable with probability p

$$\Phi_{\Delta(x,x')}(s) = (1-p) \Phi_{\Delta(x,x')|\xi=0}(s) + p \Phi_{\Delta(x,x')|\alpha=1}(s)$$

with $\Phi_{\Delta(x,x')|\alpha=1}(s) = \mathbb{E}_{\xi|\alpha=1} [\Phi_{\Delta(x,x')|\xi}(s)]$. For analytical tractability, we assume that the interference and noise term n' in (1) is Gaussian. Therefore, given ξ , $\Delta(x,x')$ is a quadratic form of the circularly symmetric complex Gaussian random vector \mathbf{z} . Using the standard result of [11], we find that

$$\Phi_{\Delta(x,x')|\xi}(s) = \frac{1}{1 + \frac{d^2}{w} \left(s - \frac{\xi + \gamma^{-1}}{w} s^2 \right)}$$

therefore

$$\text{R1: } \Phi_{\Delta(x,x')|\xi}(s) = \frac{1}{1 + \frac{d^2}{\xi + \gamma^{-1}} (s - s^2)} \quad (7)$$

$$\text{R2: } \Phi_{\Delta(x,x')|\xi}(s) = \frac{1}{1 + d^2 (s - (\xi + \gamma^{-1}) s^2)} \quad (8)$$

where $d = |x - x'|$.

Given $\alpha = 1$, we have $\xi = \beta r^b$, so the pdf of ξ is

$$f(\xi|\alpha=1) = \frac{1}{\beta B(2/b, 1)} \left(\frac{\xi}{\beta} \right)^{2/b-1} \quad (9)$$

where $B(2/b, 1) = b/2$ is the Beta function. In the case of R1

$$\Phi_{\Delta(x,x')|\alpha=1}(s) = \int_0^\beta f(\xi|\alpha=1) \frac{1}{1 + \frac{d^2}{\xi + \gamma^{-1}} (s - s^2)} d\xi$$

which, substituting (9), can be manipulated into the form

$$\begin{aligned} \Phi_{\Delta(x,x')|\alpha=1}(s) &= \frac{1}{1 + \frac{d^2}{\beta + \gamma^{-1}} (s - s^2)} \times \\ &\frac{1}{B(2/b, 1)} \int_0^1 (1-\xi)^{2/b-1} \left(1 - \frac{\beta}{\beta + \gamma^{-1}} \xi \right) \times \\ &\left(1 - \frac{\beta}{\beta + \gamma^{-1}} \frac{1}{1 + \frac{d^2}{\beta + \gamma^{-1}} (s - s^2)} \xi \right)^{-1} d\xi \quad (10) \end{aligned}$$

Invoking the identity (p.287 [12])

$$\int_0^1 x^{\lambda-1} (1-x)^{\mu-1} (1-ux)^{-\rho} (1-vx)^{-\sigma} dx = B(\mu, \lambda) F_1(\lambda, \rho, \sigma, \lambda + \mu; u, v)$$

with $\text{Re}\lambda > 0$, $\text{Re}\mu > 0$, (10) becomes

$$\begin{aligned} \Phi_{\Delta(x,x')|\alpha=1}(s) &= \frac{1}{1 + \frac{d^2}{\beta + \gamma^{-1}} (s - s^2)} \times \\ &F_1 \left(1, -1, 1, \frac{2}{b} + 1; \frac{\beta}{\beta + \gamma^{-1}}, \frac{\beta}{\beta + \gamma^{-1} + d^2 (s - s^2)} \right) \quad (11) \end{aligned}$$

where

$$F_1(\lambda, \rho, \sigma, \lambda + \mu; u, v) = \sum_{m=0}^{+\infty} \sum_{n=0}^{+\infty} \frac{(\lambda)_{m+n} (\rho)_m (\sigma)_n}{(\lambda + \mu)_{m+n} m! n!} u^m v^n$$

with $|u| < 1$, $|v| < 1$, is the first hypergeometric function of two variables and $(\lambda)_m \triangleq \lambda(\lambda+1)\dots(\lambda+m-1)$, $m > 0$, $(\lambda)_0 \triangleq 1$. Note that the first term in (11) is (7), with β in place of ξ . The second term introduces the effect of the PC adjustments on the interfering users.

When $\gamma \rightarrow \infty$, then, using the identity (p.286 [12])

$$\int_0^1 x^{\lambda-1} (1-x)^{\mu-1} (1-ux)^{-\rho} dx = B(\mu, \lambda) {}_2F_1(\rho, \lambda; \lambda + \mu; u)$$

with $\text{Re}\lambda > 0$, $\text{Re}\mu > 0$, it can easily be shown that

$$\begin{aligned} \Phi_{\Delta(x,x')|\alpha=1}^{\gamma \rightarrow \infty}(s) &= \frac{2}{2+b} \frac{1}{1 + \frac{d^2}{\beta} (s - s^2)} \times \\ &{}_2F_1 \left(1, 1; \frac{2}{b} + 2; \frac{1}{1 + \frac{d^2}{\beta} (s - s^2)} \right) \quad (12) \end{aligned}$$

where

$${}_2F_1(\rho, \lambda; \lambda + \mu; u) = \sum_{m=0}^{+\infty} \frac{(\rho)_m (\lambda)_m}{(\lambda + \mu)_m m!} u^m, \quad |u| < 1$$

is the Gauss hypergeometric function.

In the case of R2, taking the expectation of (8) over ξ gives

$$\Phi_{\Delta(x,x')|\alpha=1}(s) = \frac{1}{1 + d^2(s - (\beta + \gamma^{-1})s^2)} \times \frac{1}{B(2/b, 1)} \int_0^1 (1 - \xi)^{2/b-1} \times \left(1 + \frac{d^2 \beta s^2}{1 + d^2(s - (\beta + \gamma^{-1})s^2)} \xi\right)^{-1} d\xi$$

Employing the previous identity, we obtain

$$\Phi_{\Delta(x,x')|\alpha=1}(s) = \frac{1}{1 + d^2(s - (\beta + \gamma^{-1})s^2)} \times {}_2F_1\left(1, 1; \frac{2}{b} + 1; -\frac{d^2 \beta s^2}{1 + d^2(s - (\beta + \gamma^{-1})s^2)}\right) \quad (13)$$

Similarly to R1, the first term is (8), with ξ replaced by β , and the second term introduces the effect of the interference power variations.

IV. NUMERICAL RESULTS

Let UI be situated on the line segment between B_0 and B_1 . Unless otherwise stated, UI is at the border of the cell, i.e. $r_0 = 1$, the reuse distance is set to $D = 2$ and $b = 4$. We assume operation in the high SNR regime, setting $\gamma = 30$ dB, so that the system is completely interference limited.

The optimum rate 1/2 convolutional codes shown in table I and obtained from p.540 of [13], are combined with QPSK using Gray mapping. Error events with length up to $d_{\min} + 2$ are taken into account in (4) and the respective weights are obtained from [14]. For QPSK there is only one closest neighbor symbol error event $x \rightarrow x'$, $|x - x'| = d_{\min} = \sqrt{2}$, so $\Phi(s) = \Phi_{\Delta(d_{\min})}(s)$. For the simulations, codewords of 800 bits were used, with random bit interleaving within each codeword.

In fig.3, the BER is plotted vs. the system load. We observe that the performance gain of R1 over R2 increases as p is decreased. This is primarily because R1 makes use of the information of whether a slot is interfered or not (diversity due to hopping.) However, even at high system load ($p \geq 0.8$), where most of the slots are interfered, the gain remains substantial. This implies that the variation of the interference power due to the PC of the users of B_1 is significant enough for R1 to maintain its advantage. The simulation results reveal that the analysis is accurate; any discrepancy is due to the fact that the truncated union bound in (4) is simply an approximation to the true BER.

Another obvious observation on fig.3 is that, increasing the decoding complexity (in terms of the memory of the encoder), yields a larger performance gain for R1 than for R2. This

TABLE I
OPTIMUM RATE 1/2 CONVOLUTIONAL CODES

Encoder	Memory	$g^{(0)}$	$g^{(1)}$	d_{\min}
1	3	13	17	6
2	5	53	75	8
3	6	117	155	10

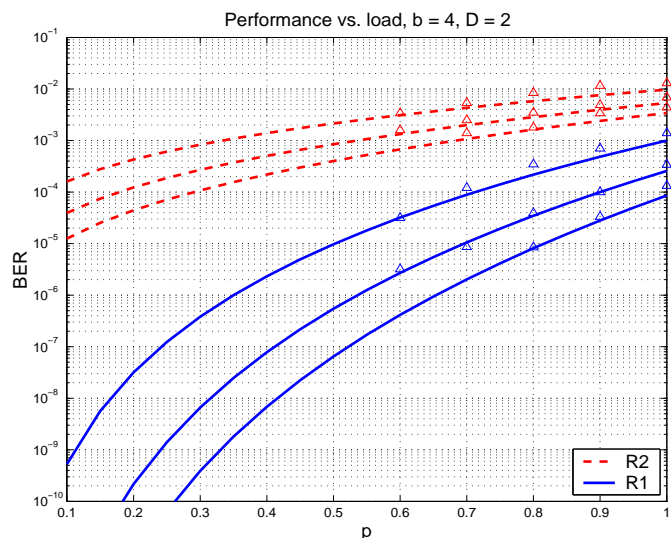


Fig. 3. Performance vs. load (analytical.) Consecutive curves of the same group correspond to Enc1, Enc2 and Enc3 in this order. Markers are simulation results.

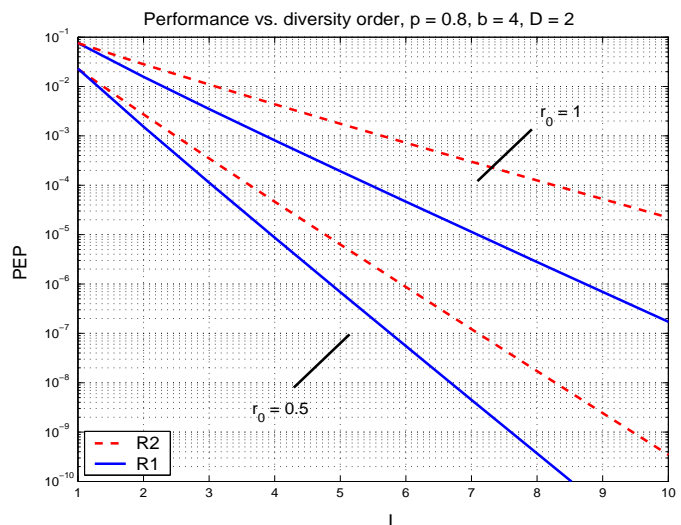


Fig. 4. Performance vs. code diversity order (analytical.)

motivates the plot in fig.4, where the PEP, $P(d_{\min})$, is plotted vs. d_{\min} for $r_0 = 0.5, 1$. A PEP value of approximately 2×10^{-4} is achieved by both a system employing a code with $d_{\min} = 5$ and R1 and a system with $d_{\min} = 7$ and R2, when $r_0 = 1$. In other words, interference can be mitigated either by increasing the decoder complexity or by adding an interference tracking capability to the receiver. The difference between the two strategies is less apparent as UI is moved closer to B_0 , whereby the long-term SIR is increased, rendering the interference power variations less important.

In fig.5, the BER is plotted vs. r_0 . Note the cross-over between the curves Enc1-R1 and Enc2-R2, Enc3-R2 at $r \simeq 0.5, 0.75$ respectively. At distances $r > 0.5(0.75)$, it is better to employ Enc1 with R1 than Enc2 (Enc3) with R2. The same

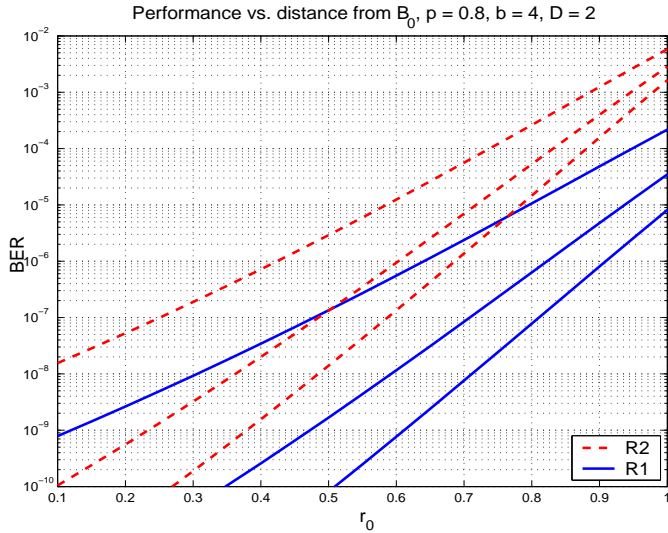


Fig. 5. Performance vs. distance of UI from B_0 (analytical.) Consecutive curves of the same group correspond to Enc1, Enc2 and Enc3 in this order.

observations can be made if r_0 is held constant and the reuse distance D becomes variable.

Finally, in fig.6 the BER is plotted vs. the path loss exponent b . As b is increased, the performance improves for both receivers. This is due to the fact that, for $R = 1$, the total interference power ξ takes smaller values, as can also be seen in fig.2. It is evident that the BER decreases faster for R1 compared to R2.

V. CONCLUSIONS

Interference diversity is inherently present in systems that utilize FH and PC. In this paper, we examined the advantages of tracking vs. ignoring the interference power variations in a downlink setting, considering a channel model with fading and path loss. We verified that providing interference information to the decoder is beneficial for the performance, even at a high load. For small long-term SIRs, which correspond to the user being situated close to the boundary of its cell and thus to other base-stations, it was found preferable to trade decoding complexity (in terms of the encoder memory) with an interference tracking capability. Concluding, we would like to point out that our analysis enables the evaluation of the BER for any combination of long-term random variables, such as r_0 or R , or parameters such as b , D and L . The operating mode of the receiver (R1 or R2) can then be selected accordingly.

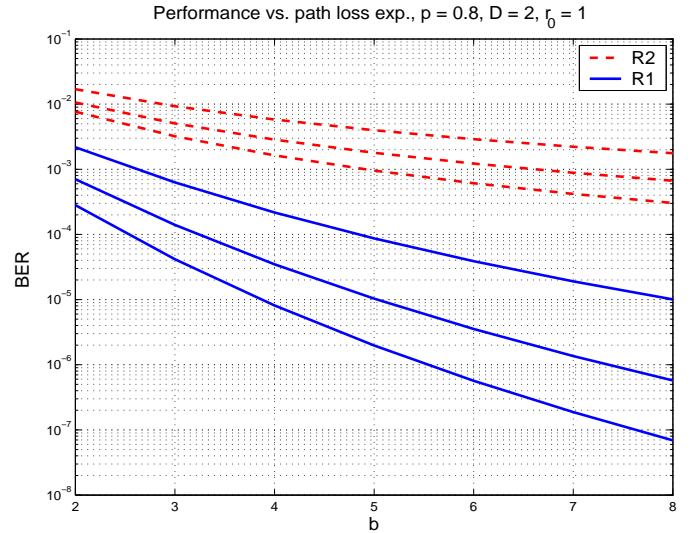


Fig. 6. Performance vs. path loss exponent (analytical.) Consecutive curves of the same group correspond to Enc1, Enc2 and Enc3 in this order.

REFERENCES

- [1] C. W. Baum and M. B. Pursley, "Bayesian methods for erasure insertion in frequency-hop communication systems with partial band interference," *IEEE Trans. Commun.*, vol. 40, pp. 1231–1238, July 1992.
- [2] S. Bruck, "Modelling interference diversity in GSM networks," in *Proc. VTC*, vol. 1, Sept. 2000, pp. 24–28.
- [3] G. J. Pottie and A. R. Calderbank, "Channel coding strategies for cellular radio," *IEEE Trans. Veh. Technol.*, vol. 44, pp. 763–770, Nov. 1995.
- [4] R. Laroia, S. Uppala, and J. Li, "Designing a mobile broadband wireless access network," *IEEE Signal Processing Mag.*, pp. 20–28, Sept. 2004.
- [5] H. Olofsson, J. Näslund, and J. Sköld, "Interference diversity gain in frequency hopping GSM," in *Proc. VTC*, vol. 1, Aug. 1995, pp. 102–106.
- [6] M. Chiani, E. Agrati, M. Mezzetti, and O. Andrisano, "Frequency and interference diversity in slow frequency hopping mobile radio systems," in *Proc. PIMRC*, vol. 2, Oct. 1996, pp. 648–652.
- [7] K. Stamatiou and J. G. Proakis, "A performance analysis of coded frequency-hopped OFDMA with imperfect channel estimation," in *Proc. IEEE PIMRC*, Sept. 2005.
- [8] G. Caire, G. Taricco, and E. Biglieri, "Bit-interleaved coded modulation," *IEEE Trans. Inform. Theory*, vol. 44, pp. 927–946, May 1998.
- [9] A. K. Gupta and S. Nadarajah, *Handbook of Beta distribution and its applications*, 1st ed. Marcel Dekker, 2004.
- [10] E. Biglieri, G. Caire, G. Taricco, and J. Ventura-Traveset, "Simple method for evaluating error probabilities," *IEEE Electron. Lett.*, vol. 32, pp. 191–192, Feb. 1996.
- [11] G. L. Turin, "The characteristic function of hermitian quadratic forms in complex normal variables," in *Biometrika*, vol. 47.
- [12] I. S. Gradshteyn and I. M. Ryzhik, *Table of integrals, series and products*, 4th ed. Academic Press, 1980.
- [13] S. Lin and D. J. Costello, *Error control coding*, 2nd ed. Prentice Hall, 2004.
- [14] J. Conan, "The weight spectra of some short low-rate convolutional codes," *IEEE Trans. Commun.*, vol. 32, pp. 1050–1053, Sept. 1984.